COMPARATIVE ANALYSIS OF SINGULAR VALUE DECOMPOSITION AND EIGEN VALUE DECOMPOSITION BASED PRINCIPAL COMPONENT ANALYSIS FOR EARTH AND LUNAR HYPERSPECTRAL IMAGE

Prateek Tripathi, Rahul Dev Garg

Geomatics Engineering, Department of Civil Engineering, Indian Institute of Technology, Roorkee 247 667, India

ABSTRACT

Data dimensionality reduction is a sensitive issue in the hyperspectral image processing. Hyperspectral imageries with hundreds of contiguous bands, have lot of redundant information. Data dimensionality reduction techniques used for hyperspectral imageries varies in the terms of decomposition method used. This paper discusses about a comparative analysis of Singular Value Decomposition (SVD) and Eigen Value Decomposition (EVD) based principal component analysis for PRISMA and Moon Mineralogy Mapper hyperspectral imageries. It is found that both methods have their own advantages. PCA with Eigen value Decomposition and lower correlation between different bands, can be used for deriving various band ratios, which facilitates a better mineral mapping. The newly launched PRISMA datasets shows sufficient results for minerals when compared to lithological map.

Index Terms— Principal Component Analysis, Eigen Value Decomposition, Singular Value Decomposition, Hyperspectral Image, Data Dimensionality

1. INTRODUCTION

Hyperspectral Image gives detailed spectral information that can be used for many applications in agricultural analysis, geological mapping, mineral exploration, forestry, water resources.

Dimensionality reduction for hyperspectral remote sensing is a vital preprocessing step and very useful in scientific applications. Hyperspectral data with hundreds of contiguous bands and narrow bandwidth, captures the information about a LULC (land use and land cover) scene in the extended wavelength of 400-2500 nm. The natural features like vegetation, soil rarely show a large deviation in their spectral features within the range of 5-10 nm. In these type of datasets various bands contains similar information due to narrow bandwidth (5 to 10 nm) leading to the redundancy in datasets. This redundancy should be reduced without hampering the quality of actual data [1]–[5].

Data dimensionality reduction methods are also used as a preprocessing step for the machine learning problems such as clustering and classification. The number of bands in any datasets governs the accuracy of classification, hence will be very vital in generating comprehensive models at a low computational cost [6]–[8].

With emerging trends in Hyperspectral remote sensing, free datasets from various airborne and space borne sensors are available. The emerging and new machine learning algorithms has evolved the high dimensional remote sensing data, i.e., Hyperspectral data for dimensionality reduction. There are many data dimensionality reduction techniques available including Principal Component Analysis (PCA), Minimum Noise Fraction (MNF, Independent Component Analysis and many more. Principal Component Analysis (PCA) is one of the most used data dimensionality reduction techniques used for Hyperspectral datasets. It represents the low dimensional form of a high dimensional datasets. One of the most important steps of PCA is to decompose the matrix (pixels in image) to different components on the basis of either covariance or correlation. PCA projects the data into a new dimension. There are various methods for decomposition of a matrix but here Eigen Value decomposition (EVD) and Singular value decomposition (SVD) methods are discussed. These decomposition methods differ on the basis of vectors used, which also defines the new subspace. SVD uses the orthogonal vector while the value of diagonal matrix in Eigen decomposition can be complex number. SVD can be calculated for the rectangular and square matrix both, whereas the Eigen decomposition can only be calculated for square matrices, and sometimes it doesn't exist for square matrix too [9]–[12]. Various features like vegetation area, water body and hills can be seen in different Principal components. PCA is earlier used for mineral mapping by various researchers. This work will check the dominance of a particular feature with respect to covariance and correlation.

Earth observation and Lunar hyperspectral data are used in this work for a comparative analysis of both decomposition methods.

2. METHODS AND MATERIALS

This work utilizes the PRISMA (PRecursore IperSpettrale della Missione Applicativa), which is a space borne hyperspectral sensor which provides imageries of the Earth's surface with (i) global coverage of 30 km × 30 km with a total acquisition capacity of 1800 km in a continuous strip, and (ii) spectral resolution of 12 nm for the contiguous bands (400–2500 nm wavelength) [13]. PRISMA is the new and free to access datasets with the best SNR and largest swath [14],[15]. PRISMA datasets for Sithampoondi, Namakkal District, Tamil Nadu (11°24′ N, 77° 92′ E) have been used in this work. This work also compares the both decomposition methods for the lunar hyperspectral data from Moon Mineralogy Mapper (M^3) sensor onboard ISRO's Chandrayaan-1 spacecraft with spatial resolution of 140 m/pixel globally and doubled from 200 km orbit, spectral coverage of 446-3000 nm (86 bands) with a swath of 40km. It has a spectral resolution in the range of 20-40 nm [16]. M^3 data for Hutton impact crater with other nearby craters (37° 18′ N, 168° 42′ E), on the far side of the Moon have been used in this work. PCA is applied on all these datasets and checked for mineral mapping.

PCA can be expressed as a presentation of original data in fewer dimensions. In first step the image data is scaled using mean and centering all the elements. Further the similarity analysis has been formed using covariance and correlation methods for the scaled data. Correlation shows how two columns change with respect to each other in terms of amplitude and direction (Positive and negative) whereas Covariance checks correlation across multiple columns. Decomposition will give more insights about the datasets The covariance matrix then decomposed to principal component using one of the decomposition method either EVD or SVD (Fig. 1). Considering an Image as a matrix of mXn dimensions, the EVD and SVD are described in the next sections [17], [18].

2.1 Eigen Vector Decomposition (EVD)

EVD of a square matrix results into a set of eigenvectors and eigenvalues [19]. Suppose M is an n X n parent square Matrix, then

$$M.EVT= \lambda. EVT \quad\text{………….…..(1)}$$

Here EVT is a non-zero n X 1 vector and λ is a scalar, which may be either real or complex. Eigen value also called as characteristic value if for any value of λ, the Eq. (1) has a solution. It is sometimes also called the characteristic value. In this case, Eq. (1) can be written as

$$M.EVT - \lambda. EVT=0$$
$$M.EVT - \lambda. I.EVT=0$$
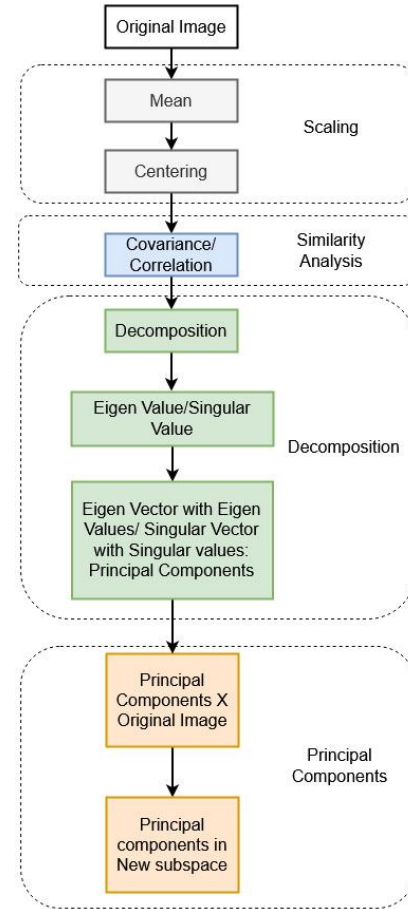$$(M- \lambda. I). EVT=0$$

Fig. 1 Flow diagram for a Basic Principal Component Analysis Technique

Here EVT cannot be a zero vector and I is an identity matrix with ones at the diagonal and other as zero,

$$|M- \lambda\cdot I|=0 \quad\text{………………….….(2)}$$

The roots of this equation (2) are called the eigenvalues of A. For each eigenvalue there exist an eigenvector for which the characteristic equation (2) is true.

2.2 Singular Value Decomposition (SVD)

SVD is an attractive and emerging algebraic algorithm for image processing algorithms. SVD can factorize a real or a complex matrix, not necessarily square similar to the symmetric or Hermitian square diagonal matrices using an Eigen/singular vectors. It is an effective method to separate the parent matrix into a set of linearly independent matrices [17], [20], [21]. SVD decomposes the matrix on the basis of increasing variance, hence give an insight about the nature of matrix. Consider an m X n matrix M (parent) such that,

$$M= U\Sigma V^T$$

Where Σ is a diagonal matrix with the singular values of parent matrix M, which can be calculated as the square root of Eigen Vectors of $M.M^T$ or $M^T.M$ (both). Both $M.M^T$ or $M^T.M$ are square, symmetrical, have same eigenvalues as zero or positive, and same rank as of parent matrix. U and V are orthogonal matrices where U is an m X m matrix and V is an n X n matrix. Image compression, optimal sub rank approximations on decompositions are few properties of Singular value decomposition.
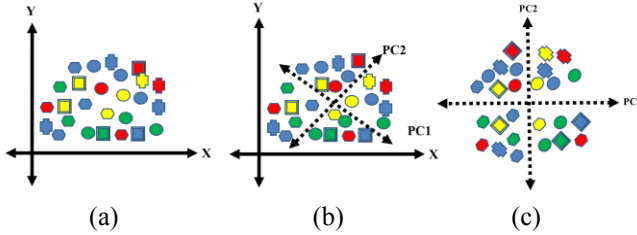

(a)   (b)   (c)

Fig. 2 Data Dimensionality reduction in a 2D space using principal Component Analysis (a) Original data (b) New axis assigned on the basis of correlated variables (c) Principal Components in anew subspace

The Eigen and Scalar vectors with the values obtained, also known as principal components (PC), are then sorted in descending order to assign a rank. They later know as principal component 1 and so on. A total of n or less vectors or components with largest values must be selected to project into a chosen subspace (Fig. 2). Both of these decomposition methods can be reversed to construct parent matrix.

3. DISCUSSIONS

3.1 Technical Details

Principal Component analysis using EVD and SVD implemented using Python and Exelis ENVI Geospatial software. Numpy, GDAL, matplotlib, scipy, panda, sklearn, skimage, spectral, cv2 libraries were used in Python.

For calculation of PCA:
    pca = PCA(n_components=5)
      #pca.fit (<Image array>)

For Singular Value Decomposition:
    <U, Σ, V >= np.linalg.svd(Image 2-D array)
    SVDPCA = np.array(np.dot(U*Σ,V),dtype=float)

Reconstruction of matrix:
    Reduced Image = U.dot(Σ.dot(V))

The PCA components obtained after applying EVD can be seen in Fig. 3(a, b, c) with true color composite in Fig 3d.

Striping error is more evident PC4 and PC5 while it is absent in the PC obtained through SVD as shown in Fig. 3 (e, f). Although the features like vegetation, hill, urban features and road are more clear in PC obtained through EVD 1 and 4 when compared to Fig. 3d. False color composite created and shown in Fig. 4(b and c), are also helpful in delineating the linear feature and differentiate the vegetation above the hills and agricultural fields near to urban area, when compared to Fig. 4a.
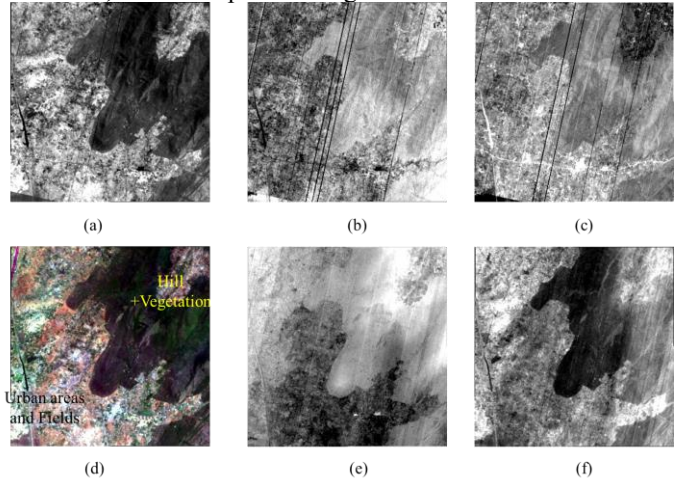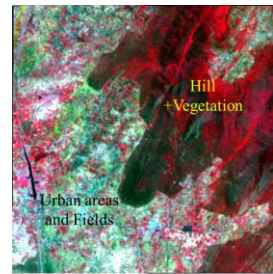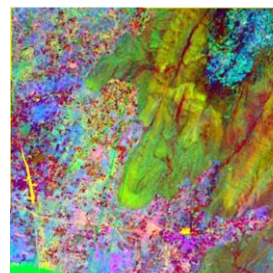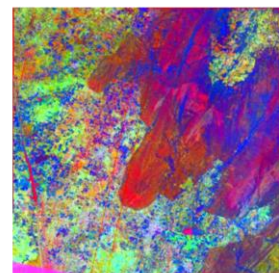

Fig. 3 PRISMA datasets (a) PC-EVD 1 (b) PC-EVD4 (c) PC-EVD5 (d) True color composite (TCC) with R=36, G=47, B=58 (e) PC-SVD3 (f) PC-SVD5

Fig. 4 PRISMA datasets (a) False color composite (FCC) with R=15, G=35, B=47 (b) R=PCA-EVD3, G= PCA-EVD2, B= PCA-EVD1 (c) R= PCA-EVD5, G= PCA-EVD2, B= PCA-EVD1
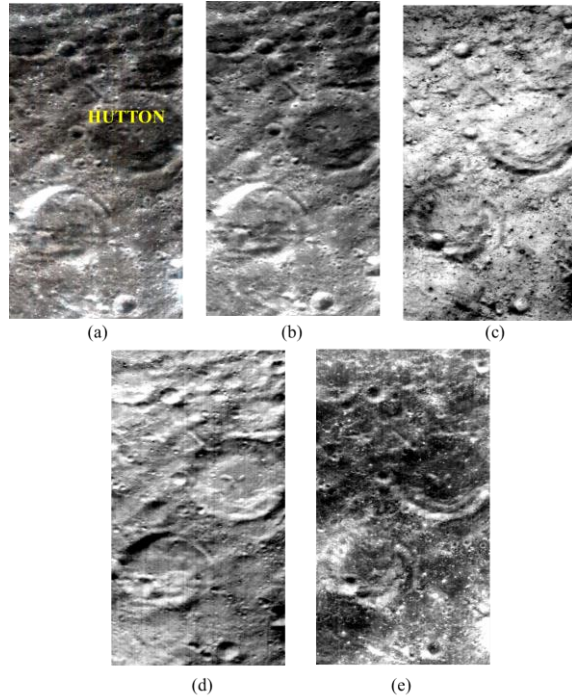
Fig. 5 M³ Image (a) False color composite with R=14 G=6 B=3 (a) PC-EVD1 (b) PC-EVD2 (c) PC-SVD2 (d) PC-SVD2
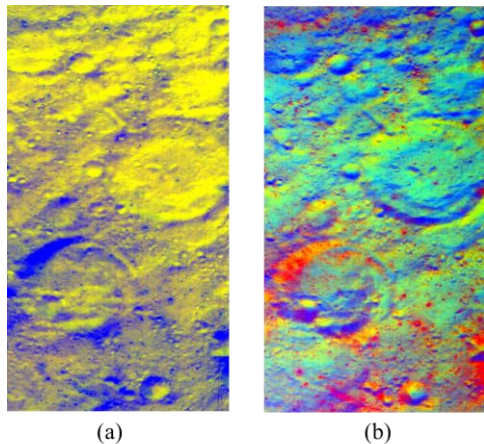

Fig. 6 M³ Image (a) Integrated Band Depth (IBD) for Hutton Crater (b) R= PC-EVD1 G= PC-EVD2 B= PC-SVD 2

For lunar hyperspectral data, PC-SVD2 in Fig. 5c, showing the very small craters as black spots. Also the depth of the impact craters near Hutton also giving a lot of information about the surface which is not visible in FCC (Fig. 5 a). Fig 5b improves the overestimation of eject and reflectance on the bottom of the image. Fig. 5(c, d and e) are showing the

ejects rays and enhancing the small impact craters and depth details for craters. For M³, SVD is showing more information as compared to EVD.

IBD helps in providing the fundamental mineralogical properties of the lunar surface by representing the area which is having mafic silicates, showing soil maturity and space weathering [22]. IBD (Integrated Band Depth) maps show the possible olivine-bearing /high mafic minerals in green-yellow color and the blue color for anorthosite or weathered minerals at Highlands (Fig. 6a). The FCC generated and shown in the image (Fig. 6b), when compared to IBD gives an idea about the mineralogy of the surface.

4. CONCLUSION

PCA with both the decomposition methods shows the satisfactory results. The SVD reduces the noise and give more accurate outputs. Both SVD and EVD based PCA can be used to generate band ratios. These band ratios can be very helpful in mineral mapping. PCA for lunar hyperspectral data, can guide for a better and accurate spectral analysis. The spectra from the lunar surface or craters, can be extracted after analyzing the results from PCA. The future work will include the compression of newly launched PRISMA hyperspectral datasets. A kernel based normalized PCA using SVD decomposition technique is in progress.

6. REFERENCES

[1]   E. Ben-Dor, D. Schläpfer, A. J. Plaza, and T. Malthus, "Hyperspectral Remote Sensing," *Airborne Meas. Environ. Res. Methods Instruments*, pp. 413–456, 2013.

[2]   F. van der Meer, "The effectiveness of spectral similarity measures for the analysis of hyperspectral imagery," *Int. J. Appl. Earth Obs. Geoinf.*, vol. 8, no. 1, pp. 3–17, 2006.

[3]   B. M., William, HungateS., and Watkins R., "Hyperspectral remote sensing," *Guang Pu Xue Yu Guang Pu Fen Xi*, vol. 30, no. 10, pp. 2724–8, 2010.

[4]   R. N. Sahoo, "Hyperspectral Remote Sensing," *Indian Agric. Stat. Res. Institute, New Delhi 110 012.*, vol. 110, no. Figure 1, pp. 107–129, 2013.

[5]   V. Sivakumar, R. Neelakantan, and M. Santosh, "Lunar surface mineralogy using hyperspectral data: Implications for primordial crust in the Earth–Moon system," *Geosci. Front.*, vol. 8, no. 3, pp. 457–465, 2017.

[6]   H. N. D. Le, M. S. Kim, and D.-H. Kim, "Comparison of singular value decomposition and

principal component analysis applied to hyperspectral imaging of biofilm," in *IEEE Photonics Conference 2012*, 2012, pp. 6–7.

[7]   C. Rodarmel and J. Shan, "Principal component analysis for hyperspectral image classification," *Surv. L. Inf. Sci.*, vol. 62, no. 2, pp. 115–122, 2002.

[8]   J. C. Harsanyi and C.-I. Chang, "Hyperspectral image classification and dimensionality reduction: An orthogonal subspace projection approach," *IEEE Trans. Geosci. Remote Sens.*, vol. 32, no. 4, pp. 779–785, 1994.

[9]   J. A. Richards, *Remote sensing digital image analysis: An introduction*, vol. 9783642300622. Springer, 2013.

[10]   A. P. Cŕosta, C. R. De Souza Filho, F. Azevedo, and C. Brodie, "Targeting key alteration minerals in epithermal deposits in Patagonia, Argentina, using ASTER imagery and principal component analysis," *Int. J. Remote Sens.*, vol. 24, no. 21, pp. 4233–4240, 2003.

[11]   A. P. Crosta and J. M. Moore, "Enhancement of Landsat thematic mapper imagery for residual soil mapping in SW Minas Gerais state Brazil : a prospecting case history in Greenstone belt terrain," *Proc. 7th Themat. Conf. Remote Sens. Explor. Geol.*, vol. Calgary, no. 2-6 Oct, pp. 1173–1187, 1989.

[12]   W. P. Loughlin, "Principal component analysis for alteration mapping," *Photogramm. Eng. Remote Sens.*, vol. 57, no. 9, pp. 1163–1169, 1991.

[13]   P. Tripathi and R. D. Garg, "First Impressions from the PRISMA Hyperspectral Mission," *Curr. Sci.*, vol. 19, no. October, pp. 1267–1281, 2020.

[14]   Christiano Contini, "PRISMA Space Segment," in *First National Workshop on Data Exploitation of PRISMA Mission Precursor of National Hyperspectral Space Mission Italian Space Agency (ASI)*, Mar. 2007, pp. 1–12, .

[15]   R. Loizzo *et al.*, "Prisma: The Italian hyperspectral mission," in *International Geoscience and Remote Sensing Symposium (IGARSS)*, Oct. 2018, vol. 2018-July, pp. 175–178.

[16]   C. M. Pieters *et al.*, "The Moon mineralogy mapper (M3) on Chandrayaan-1," *Curr. Sci.*, vol. 96, no. 4, pp. 500–505, 2009.

[17]   R. A, "SVD Based Image Processing Applications: State of The Art, Contributions and Research Challenges," *Int. J. Adv. Comput. Sci. Appl.*, vol. 3, no. 7, pp. 26–34, 2012.

[18]   C. I. Chang, "Interference and noise-adjusted principal components analysis," *IEEE Trans. Geosci. Remote Sens.*, vol. 37, no. 5 II, pp. 2387–2396, 1999.

[19]   L. Annala, M. A. Eskelinen, J. Hämäläinen, A. Riihinen, and I. Pölönen, "Practical approach for hyperspectral image processing in Python," *Int. Arch. Photogramm. Remote Sens. Spat. Inf. Sci. - ISPRS Arch.*, vol. 42, no. 3, pp. 45–52, 2018.

[20]   L. Cao, "Singular Value Decomposition Applied To Digital Image Processing," pp. 1–15.

[21]   C. J. Ogden and T. Huff, "The Singular Value Decomposition and Its Applications in Image Processing," no. December, p. 12, 1997.

[22]   J. F. Mustard *et al.*, "Compositional diversity and geologic insights of the Aristarchus crater from Moon Mineralogy Mapper data," *J. Geophys. Res. E Planets*, vol. 116, no. 5, pp. 1–17, 2011, doi: 10.1029/2010JE003726.